J Solid State Electrochem (2012) 16:1323–1331
DOI 10.1007/s10008-011-1526-1

ORIGINAL PAPER

Simultaneous determination of catechol and hydroquinone based on poly (diallyldimethylammonium chloride) functionalized graphene-modified glassy carbon electrode

Letao Wang · Yan Zhang · Yongling Du · Daban Lu · Yuzhen Zhang · Chunming Wang

Received: 7 July 2011 / Revised: 3 August 2011 / Accepted: 5 August 2011 / Published online: 19 August 2011

Abstract Simultaneous determination of catechol (CC) and hydroquinone (HQ) were investigated by voltammetry based on glassy carbon electrode (GCE) modified by poly (diallyldimethylammonium chloride) (PDDA) functionalized graphene (PDDA-G). The modified electrode showed excellent sensitivity and selectivity properties for the two dihydroxybenzene isomers. In 0.1 mol/L phosphate buffer solution (PBS, pH 7.0), the oxidation peak potential difference between CC and HQ was 108 mV, and the peaks on the PDDA-G/GCE were three times as high as the ones on graphene-modified glass carbon electrode. Under optimized conditions, the PDDA-G/GCE showed wide linear behaviors in the range of 1×10^{-6}–4×10^{-4} mol/L for CC and 1×10^{-6}–5×10^{-4} mol/L for HQ, with the detection limits 2.0×10^{-7} mol/L for CC and 2.5×10^{-7} mol/L for HQ (S/N=3) in mixture, respectively. Some kinetic parameters, such as the electron transfer number (n), charge transfer coefficient (α), and the apparent heterogeneous electron transfer rate constant (k_s), were calculated. The proposed method was applied to simultaneous determine CC and HQ in real water samples of Yellow River with satisfactory results.

Keywords Catechol · Hydroquinone · Graphene · PDDA · Simultaneous determination

Electronic supplementary material The online version of this article (doi:10.1007/s10008-011-1526-1) contains supplementary material, which is available to authorized users.

L. Wang · Y. Zhang · Y. Du · D. Lu · Y. Zhang · C. Wang (✉)
Department of Chemistry, Lanzhou University,
Lanzhou 730000, People's Republic of China
e-mail: wangcm@lzu.edu.cn

Introduction

As important industrial raw and processed materials, phenolic compounds catechol (CC) and hydroquinone (HQ) are widely used in photography, dyes, cosmetics, and chemical and pharmaceutical industries. Because of high toxicity and low degradability, CC and HQ are considered as environmental pollutants by the US Environmental Protection Agency (EPA) and the European Union (EU) [1]. Furthermore, due to their similar structures and characteristics, CC and HQ usually coexist and interfere with each other during their identification. Therefore, it is crucial to develop a simultaneous, simple, and rapid analytical method for the detection of dihydroxybenzene isomers. Presently, numerous methods have been established for the determination of the two compounds, including liquid chromatography [2, 3], synchronous fluorescence [4], chemiluminescence [5, 6], spectrophotometry [7], gas chromatography/mass spectrometry [8], pH-based flow injection analysis [9], electrochemical methods [10–28], etc. Among these techniques, the electrochemical methods have attracted considerable attentions due to the advantages of fast response, low cost, simple operation, and high sensitivity. Thus, many efforts have been devoted to the simultaneous determination of CC and HQ by electrochemical methods. For instance, CC and HQ were determined by using glassy carbon electrode (GCE) in micellar solutions, and the oxidation peaks for the two compounds appeared at 350 and 450 mV, respectively [13]. Additionally, CC and HQ can also be simultaneously determined on mesoporous carbon CMK-3 electrode with high sensitivity and the peak-to-peak separation of the oxidation potential was 125 mV [20]. Recently, simultaneous determination of CC and HQ had been performed at

PASA/MWNTs composite film [17] and graphene-modified GCE [26].

As a new member of the carbon family, two-dimensional carbon material graphene has attracted much attention for both fundamental research and technological applications. Graphene has a lot of advantages, such as high conductivity and superior mechanical and electronic properties, producing promising potential applications in sensors and electrocatalysis [29–32]. However, graphene is hydrophobic and tends to form agglomerates which may limit its further applications [33]. Particularly in electrochemical sensors, the prevention of aggregation is of vital importance for graphene because most of its unique properties are only associated with individual sheets [34]. Therefore, the material, which is able to prevent graphene from aggregating, has received increasing interest nowadays. Poly (diallyldimethylammonium chloride) (PDDA) is a linear positively charged polyelectrolyte, and it has been found to be attractive for functionalizing nanomaterials [35]. Thus, PDDA might be used to noncovalently functionalize graphene sheet. Additionally, PDDA has excellent binding capability with graphene and could maintain the electronic structure of graphene [34]. Therefore, the graphene functionalized by PDDA could be an effective method to increase the solubility in water.

In this work, the PDDA-functionalized graphene-modified glassy carbon electrode (PDDA-G/GCE) was employed for simultaneous determination of CC and HQ. Electrochemical behaviors of CC and HQ on modified electrode were investigated by using cyclic voltammetry (CV) and differential pulse voltammetry (DPV) method. Experimental results indicated that the two isomers of dihydroxybenzene can be simultaneously determined. The low detection limit and wide linear range were obtained on the modified electrode, and the kinetic parameters showed that this modified electrode was superior to some reported electrode. The proposed electrode was successfully applied to CC and HQ detection in the real samples of Yellow River without previous chemical or physical separations, and obtained good recoveries.

Experimental

Reagents and apparatus

CC and HQ were obtained from Tianjin Guangfu Chemical Research Institute (Tianjin, China http://www.guangfu-chem.com). Graphite powder (KS-10) and PDDA (20%) were purchased from Sigma Co (St. Louis, MO, USA http://www.sigma-aldrich.com/). Hydrazine hydrate was from Nanjing Reagent Co. Ltd (Nanjing, China http://www.nj-reagent.com). All other chemicals were of analytical grade and used without further purification. All solution was prepared with ultrapure water. Phosphate buffer solution (PBS, 0.1 mol/L) was prepared by mixing the stock solution of 0.10 mol/L NaH_2PO_4 and 0.1 mol/L Na_2HPO_4, and the pH was adjusted by NaOH or H_3PO_4; 0.10 mol/L stock solution of CC or HQ was freshly prepared by dissolving CC or HQ in boiling water and kept at 4 °C. The stock solution was diluted to various concentrations by mixing with the buffer solution.

Electrochemical measurements were performed on a CHI 1210A workstation (Shanghai Chenhua, China) with a conventional three-electrode system comprised of a platinum wire auxiliary electrode, a saturated calomel electrode as reference electrode and the modified or bare glass carbon working electrode. The morphology of the samples was observed using field-emission scanning electron microscopy (S-4800, Hitachi, Japan) and transmission electron microscopy (TEM, Tecnai G2F30, FEI, USA). X-ray diffraction (XRD) data were collected on XRD-6000 (Shimadzu, Tokyo, Japan) using Cu-Kα (1.5406 Å) radiation. The ultrapure water was prepared by the Milli-Q system (Millipore Inc. nominal resistivity 18.2 MΩ cm). All pH measurements were performed using a pHs-3B digital pH-meter (Shanghai Lei Ci Device Works, Shanghai, China).

Synthesis of the functionalized graphene and electrode preparation

Graphite oxide (GO) was synthesized from graphite powder by using the modified Hummers method [36]. One hundred milligrams of GO was dispersed in water (100 mL) to obtain a yellow-brown dispersion by ultrasonication for 12 h, then by centrifugation to remove any unexfoliated GO. Subsequently, the homogeneous GO dispersion (100 mL) was mixed with 5 mL PDDA (20%) solution and stirred for 30 min. The resulting mixture was further treated with 5 mL hydrazine hydrate and allowed to react for 24 h at 90 °C. Finally, the black PDDA-G was collected by filtration and further washed with water.

Prior to the surface modification, the bare GCE was polished with alumina slurry down to 0.05 μm, then washed successively with anhydrous alcohol and ultrapure water in an ultrasonic bath, and dried in room temperature. The PDDA-G was dissolved in ultrapure water at a concentration of 1 mg/mL with the aid of ultrasonic agitation for 6 h, resulting in a homogeneous black suspension. Afterword, 5 μL PDDA-G solution was deposited on the fresh prepared GCE surface. The electrode was dried in the room temperature. The obtained electrode was noted as PDDA-G/GCE. For comparison, graphene/GCE was fabricated with the similar procedure but the graphene was dissolved in dimethylformamide solution.

Experimental procedure

The diphenol stocking solution was diluted to the required concentration by PBS in an electrochemical cell. The water samples were prepared by adding known concentration CC or HQ in Yellow River water. Before electrochemical experiments, the solution was bubbled with nitrogen for 30 min to remove dissolved oxygen, and all the experiments were carried out at room temperature. The determination was carried out by DPV from −0.10 to 0.40 V and the DPV conditions were as follows: increment potential, 0.004 V; pulse amplitude, 0.05 V; pulse width, 0.05 s; sample width, 0.0167 s; pulse period, 0.2 s; and quiet time, 2 s.

Results and discussion

Characterization of PDDA-G

The functionalized graphene was first characterized by XRD (Fig. 1). The XRD pattern of GO (curve a) has a characteristic peak centered about at 11.0°, but the PDDA-G (curve b) appears a peak centered at 22.5°, in agreement with previous report [34], indicating that GO was reduced to graphene by hydrazine hydrate. The peak at around 43° is associated with the plane of the hexagonal structure of carbon [37]. The inset shows the image of water dispersion of graphene without (left) and with (right) PDDA. The dispersity of graphene in water was obviously improved through the noncovalent adsorption of PDDA which produce positive charge avoiding aggregation. Otherwise, the graphene would aggregate without PDDA functionalization. The morphology of functionalized graphene was characterized using TEM and SEM. The TEM (Fig. 2A) image shows transparent sheets and wrinkled flake-like shapes. Similar to the TEM image, the wrinkle can be seen clearly in the SEM image (Fig. 2B), and a nonuniform membrane with rough surface is observed. The wrinkled surface has contributions to the high surface area of PDDA-G on the electrode. The above results show that PDDA prevents the aggregation of graphene.

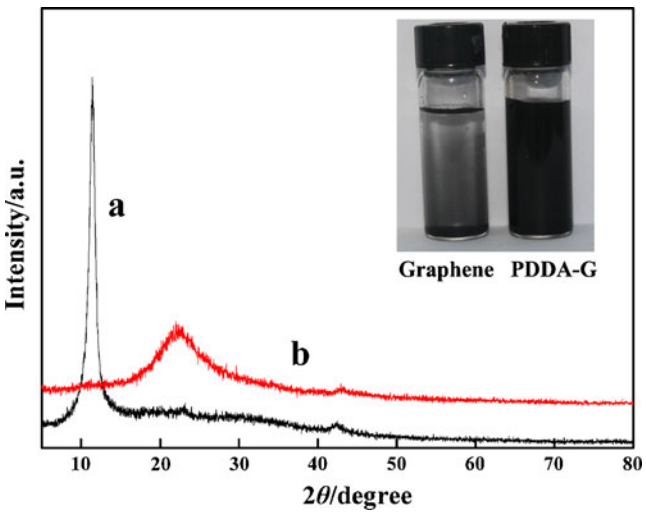

Fig. 1 XRD patterns of graphene (*a*) and PDDA-G (*b*), *inset* photo of aqueous dispersion (1 mg/mL) of graphene and PDDA-G

Electrochemical behavior of CC and HQ

The electrochemical behavior of CC and HQ on bare GCE, graphene-modified GCE, and PDDA-G/GCE were studied by using CV method. Two reduction peaks (E_{pc}), located at −0.071 and 0.053 V, respectively, were observed on the bare GCE (Fig. 3, curve a). However, only one broad oxidation peak (E_{pa}) appears at potential of 0.286 V indicating that the oxidation potential of CC and HQ overlapped at bare GCE. While at the graphene-modified GCE (curve b), two pairs of current peaks are clearly observed, which show that the oxidation and reduction peaks of CC and HQ can be separated. The oxidation peaks are at potential of 0.192 and 0.082 V, and the reduction peaks are at potential of 0.135 and 0.025 V for CC and HQ, respectively. Compared with the bare GCE, the oxidation and reduction peaks of CC and HQ can be separated completely. Compared with the graphene-modified GCE, the current peak intensities on the PDDA-G/GCE (curve c) are about three times as high. For CC, the oxidation peak and the reduction peak locate at potentials of 0.178 and 0.147 V, respectively. The potential difference (ΔE_p) is 0.031 V, smaller than the ΔE_p on the graphene-modified GCE, and reveals a faster electron transfer process on the PDDA-G/GCE. Similar to CC, the oxidation peak and the reduction peak of HQ appear at the potential of 0.08 and 0.047 V, respectively, and the corresponding ΔE_p is 0.033 V. Additionally, the oxidation peak potential difference between hydroquinone and catechol is 108 mV. These results indicate that the PDDA-functionalized graphene-modified electrode cannot only identify the CC and HQ, but also enhance the detection sensitivity.

Influence of the amount of PDDA-G

The optimal amount of PDDA-G composite solution dropped on the GCE surface was studied through the electrochemical experiment (Fig. S1 in Supplementary material). The maximum peaks of CC and HQ appeared at 5 μL. The results demonstrated that 5 μL of PDDA-G composite solution was the optimal amount.

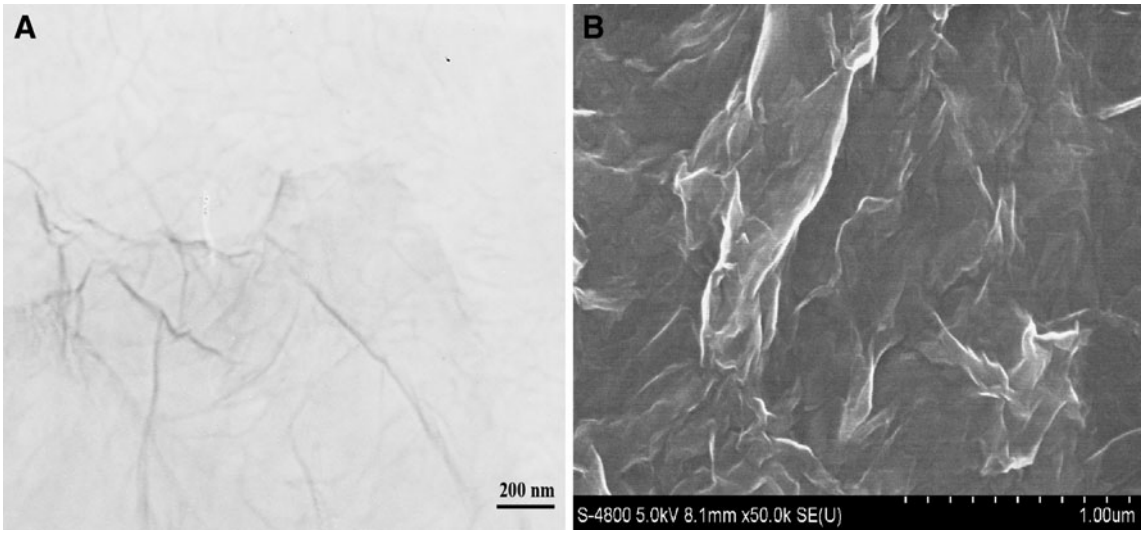

Fig. 2 The TEM (**A**) and SEM (**B**) image of as-synthesized PDDA-G

Chronocoulometry

The electrochemically effective surface areas (*A*) of graphene/GCE and PDDA-G/GCE were investigated by chronocoulometry (Fig. S2 in Supplementary material). *A* was calculated to be 0.36 cm^2 for graphene/GCE and 0.41 cm^2 for PDDA-G/GCE, indicating that PDDA prevent the aggregation of graphene sheets.

Influence of pH

The influence of pH on the electrochemical behavior of CC and HQ were carefully studied. The maximum anodic peak current appeared at pH 7.0 (Fig. 4A) for the two compounds. With the further increase of buffer solution pH, the oxidation peak current decreased obviously. This could be related to the fact that proton took part in the electrochemical reaction. When the pH value was high, the shortage of proton prevented the oxidation and reduction of CC and HQ, leading to the decrease of current peak intensity. On the other hand, the diphenol, as it is well known, tends to form anions and make the peak current decrease [26]. Therefore, pH 7.0 was selected as the optimum pH for the electrochemical detection of CC and HQ.

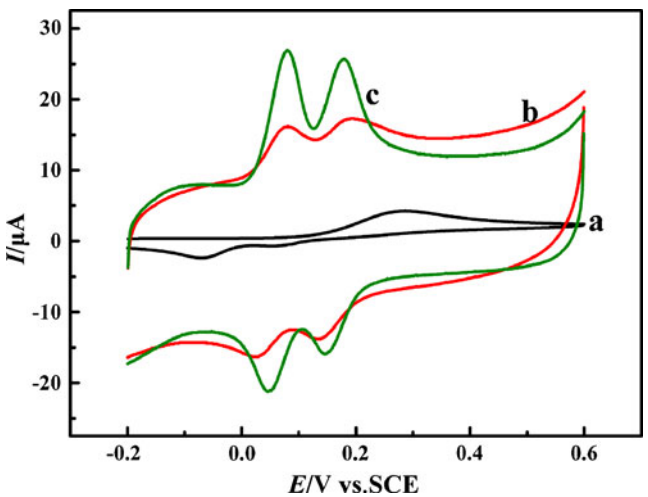

Fig. 3 Cyclic voltammograms of 1×10^{-5} mol/L CC and HQ in pH 7.0 PBS at different electrodes (*a*) GCE, (*b*) graphene (5 μL)/GCE, and (*c*) PDDA-G (5 μL)/GCE. Scan rate, 50 mV s^{-1}

In addition, in the selected pH range the formal peak potentials also negatively shift with the increase of solution pH. As shown in Fig. 4B, for CC, two linear relationships between formal peak potential and solution pH for CC were obtained in the investigated pH range: E_{pa} (V)=0.560–0.054 pH with a correlation coefficient (*R*) of 0.999 for the oxidation process and E_{pc} (V)=0.533–0.054 pH (*R*=0.999) for the reduction process. Similar to CC, for HQ the regression equations of E_{pa} (V)=0.476–0.056 pH (*R*=0.998) for the oxidation process and E_{pc} (V)= 0.441–0.057 pH (*R*=0.999) for the reduction process. The slopes of the four regression equations are close to the theory value of 58.5 mV pH^{-1}. According to the following formula [38]: $dE_p/dpH=2.303mRT/nF$, in which, *m* is the number of proton, *n* is the number of electron, and *m*/*n* is calculated to be 0.95 and 0.95 for the oxidation and reduction process of CC, respectively. Similarly, *m*/*n*=0.98 and 0.99 for the oxidation and reduction process of HQ. It indicates that the number of proton and electron involved in the electrochemical redox process of CC and HQ is equal.

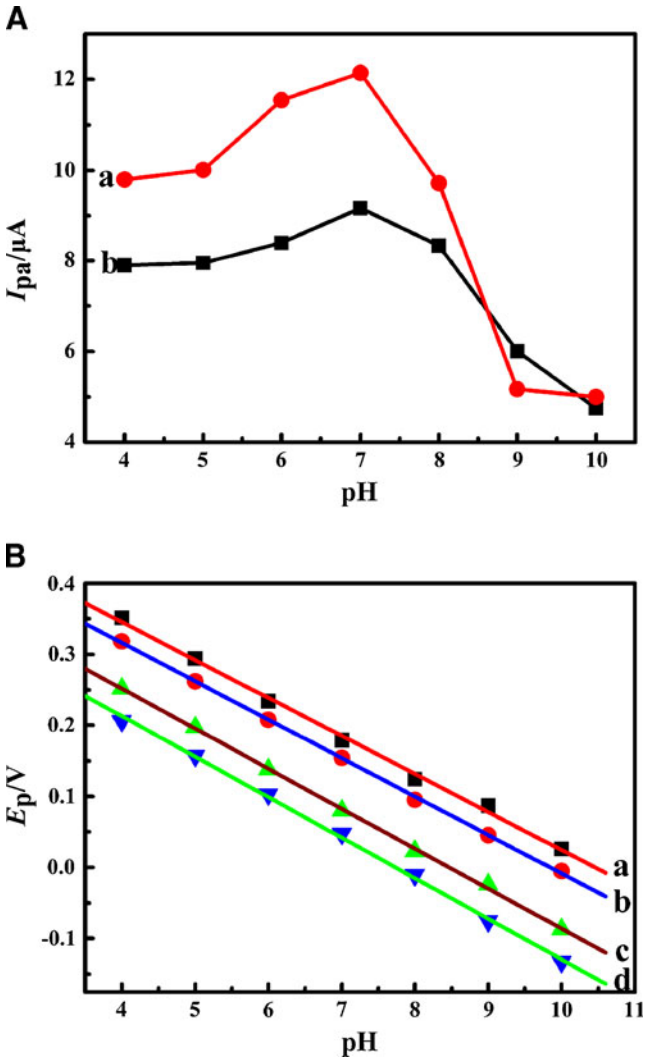

Fig. 4 Effects of pH on the oxidation peak current (**A**) and oxidation peak potential (**B**) of CC and HQ. **A** (*a*) HQ; (*b*) CC. **B** (*a*) E_{pa} of CC; (*b*) E_{pc} of CC; (*c*) E_{pa} of HQ; (*d*) E_{pc} of HQ

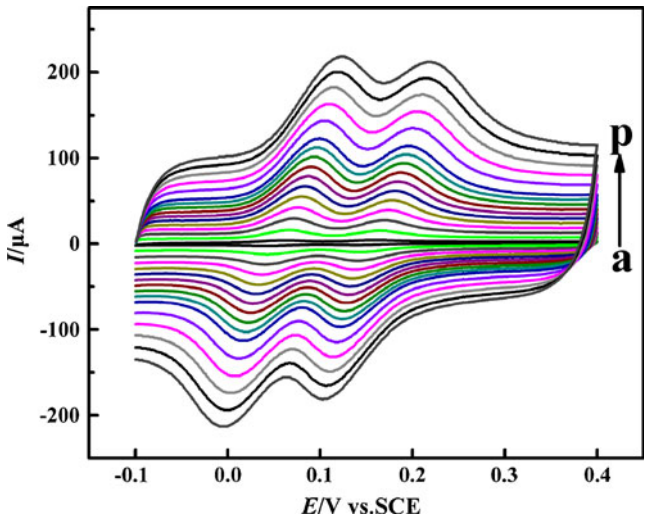

Fig. 5 Effect of scan rate on the redox behavior of 1×10^{-5} mol/L CC and HQ. (*a–p*) 10, 50, 100, 150, 200, 250, 300, 350, 400, 450, 500, 600, 700, 800, 900, and 1,000 mV s^{-1}

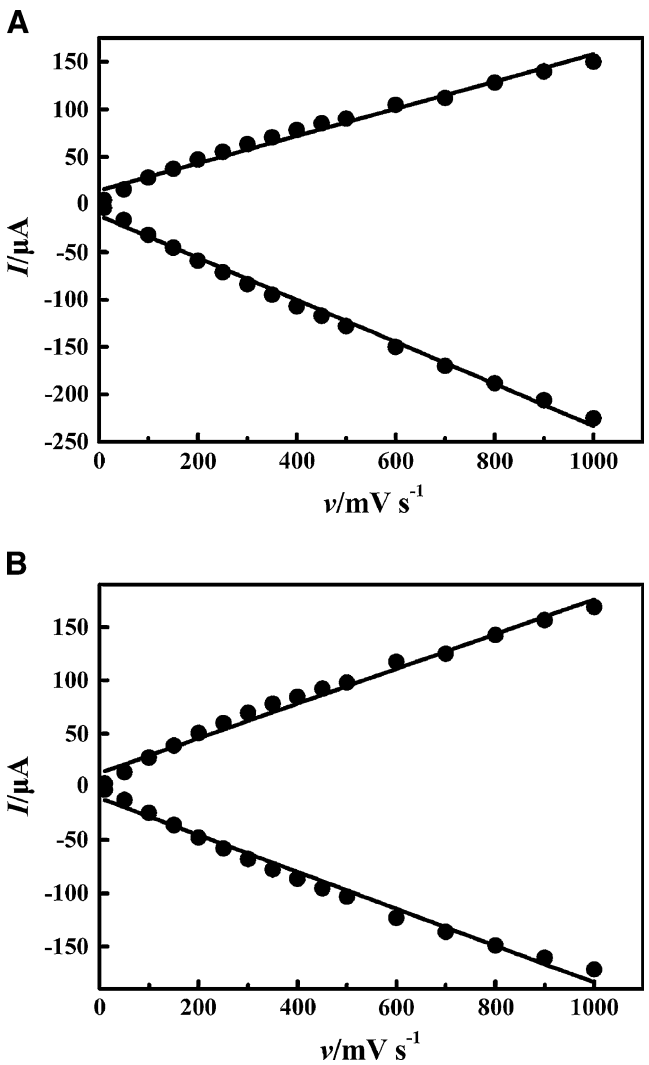

Fig. 6 The redox peak currents of CC (**A**) and HQ (**B**) vs scan rate

Influence of scan rate

To investigate the reaction kinetics, the influence of scan rate on the peak current of CC and HQ in the mixture was also investigated. As can be seen in Fig. 5, the oxidation (I_{pa}) and reduction (I_{pc}) peak currents for CC and HQ increase regularly with increase of scan rates from 10 to 1,000 mV s^{-1}. Both CC and HQ show a pair of symmetrical redox peaks. For CC (Fig. 6A), the redox peak currents follows the linear regression equation of I_{pa} (μA)=2.66+92.1 v (mV s^{-1}) and I_{pc} (μA)=−0.453–112.2 v (mV s^{-1}) with the R=0.998 and 0.999, respectively. For HQ, two linear regression were also obtained: I_{pa} (μA)=7.93+187.4 v (mV s^{-1}, R=0.993) and I_{pc} (μA)=−4.31–202.1 v (mV s^{-1}, R=0.998), respectively (Fig. 6B). As we know, linear relationship between scan rate and peak currents is the

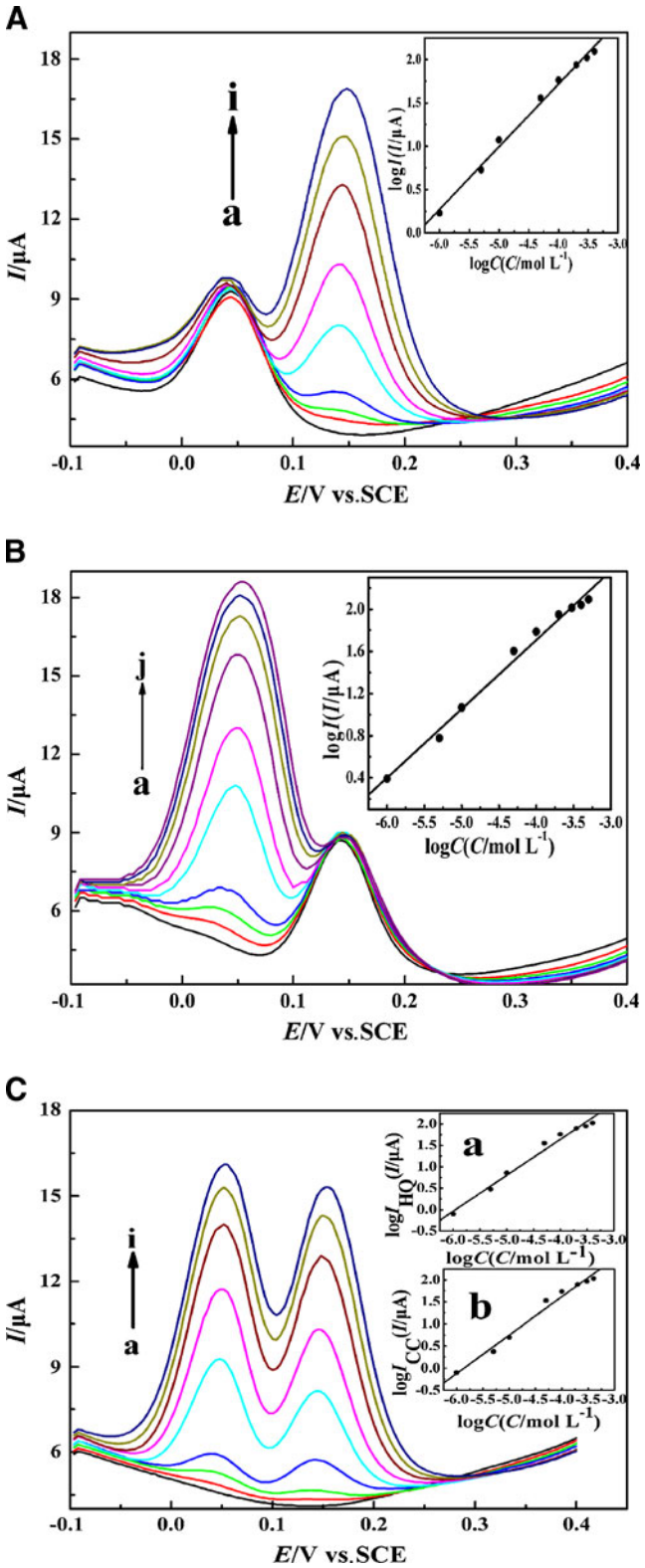

Fig. 7 **A** DPVs of CC at PDDA-G/GCE in the presence of 1×10^{-5} mol/L HQ in 0.1 mol/L PBS (pH 7.0). CC concentrations (from *a* to *i*): 0, 1×10^{-6}, 5×10^{-6}, 1×10^{-5}, 5×10^{-5}, 1×10^{-4}, 2×10^{-4}, 3×10^{-4}, and 4×10^{-4} mol/L. **B** DPVs of HQ at PDDA-G/GCE in the presence of 1×10^{-5} mol/L CC in 0.1 mol/L PBS (pH 7.0). HQ concentrations (from *a* to *j*): 0, 1×10^{-6}, 5×10^{-6}, 1×10^{-5}, 5×10^{-5}, 1×10^{-4}, 2×10^{-4}, 3×10^{-4}, 4×10^{-4}, and 5×10^{-4} mol/L. **C** DPVs of PDDA-G/GCE in 0.1 mol/L pH 7.0 PBS containing the different concentration of CC and HQ. (*a*–*i*): 0, 1×10^{-6}, 5×10^{-6}, 1×10^{-5}, 5×10^{-5}, 1×10^{-4}, 2×10^{-4}, 3×10^{-4}, and 4×10^{-4} mol/L

character of an adsorption and desorption process. Therefore, the redox process of CC and HQ on the PDDA-G/GCE is an adsorption and desorption process. However, on the graphene/GCE (Fig. S3 in Supplementary material), the peak currents are proportional to the square root of the scan rate, showing a mass diffusion-controlled process. The following reasons might explain the different results. The functionalized graphene have more functional groups than graphene, and the functional group favored the absorption of the two dihydroxybenzene isomers by electrostatic interaction.

Furthermore, the influence of scan rate on the redox peak potential was also investigated for calculating the kinetic parameters. With the increase of scan rate, the oxidation peak potential shifted positively and the reduction peak potential shifted negatively, and at higher scan rates, the anodic (E_{pa}) and cathodic (E_{pc}) peak potential showed linear relationship with the logarithm of scan rate (log(v)). For CC, two linear regression equation: E_{pa} (V)=0.221+ 0.0597 log (v) (V s^{-1}, R=0.992) and E_{pc} (V)=0.0924–0.051 log (v) (V s^{-1}, R=0.988) were obtained. For HQ, the linear relationship equation were E_{pa}(V)=0.135+0.066 log(v) (V s^{-1}, R=0.990) and E_{pc}(V)=−0.0094–0.0525 log(v) (V s^{-1}, R=0.989) for the anodic and cathodic peak potential, respectively. According to Laviron's model [38], the slope of the line for E_{pa} and E_{pc} could be expressed as $2.3RT/n$ $(1-\alpha)$ F and $-2.3RT/n\alpha F$, respectively. Therefore, for CC, the electron transfer coefficient (α) and electron transfer number (n) were calculated as 0.531 and 2, respectively. Similarly, α equals 0.558 and n equals 2 were obtained for HQ. Additionally, the apparent heterogeneous electron transfer rate constant (k_s) can also be obtained according to reference [38] based on the Eq. 1:

$$\log k_s = \alpha\log(1-\alpha) + (1-\alpha)\log\alpha - \log\frac{RT}{nFv} - \frac{\alpha(1-\alpha)nF\Delta Ep}{2.303RT} \quad (1)$$

Here, n is the number of electrons involved in the reaction, ΔE_p is the peak-to-peak potential separation, α is the charge transfer coefficient, and v is the scan rate. According to this equation, the k_s for CC were calculated as 3.85 and 3.65 s^{-1} for HQ. Furthermore, the k_s was calculated by the square-wave voltammograms [39], and the results were similar (Supplementary material).

The k_s of the graphene/GCE were calculated by Laviron's model (Supplementary material), and the result is smaller

Table 1 Performance comparison of the modified electrode for CC and HQ detection with other electrodes

Electrode	Technique	Linear range (10^{-6} mol/L)		LOD (10^{-6} mol/L)		Reference
		CC	HQ	CC	HQ	
CILE	DPV	0.5–200	0.5–200	0.5	0.2	[12]
IL-CPE	DPV	–	10–1,500	–	4	[15]
PASA/MWNTs/GCE	DPV	6–180	6–100	1	1	[17]
CMK-3-Nafion/GCE	DPV	0.5–20	0.5–25	0.1	0.1	[20]
PPABA/GCE	DPV	2–900	1.2–600	0.50	0.40	[21]
MPE	DPV	20–50	50–2,000	–	–	[23]
Graphene/GCE	DPV	1–50	1–50	0.015	0.01	[26]
Graphene–chitosan/GCE	DPV	1–400	1–300	0.75	0.75	[28]
CCM-CPE	Amperometry	–	0.1–137.5	–	0.05	[40]
PDDA-G/GCE	DPV	1–400	1–500	0.20	0.25	This work

PASA poly-amidosulfonic acid, *CILE* carbon ionic liquid electrode, *MWNTs* multi-wall carbon nanotubes, *PPABA* poly(*p*-aminobenzoic acid), *CCM-CPE* core-shell magnetic nanoparticles supported on carbon paste electrode, *IL-CPE* ionic liquid modified carbon paste electrode, *MPE* mesoporous platinum electrode, *DPV* differential pulse voltammetry

than the PDDA-G/GCE, indicating the PDDA-functionalized graphene film can effectively promote the electron transfer.

Simultaneous determination CC and HQ

The above investigations indicated that PDDA-G/GCE exhibited obvious electrocatalytical effect to the oxidation of CC and HQ. Subsequently, DPV was employed to investigate the simultaneous determination of CC and HQ. The principle of measurement was based on the individual determination of CC, or HQ in their mixtures when the concentration of one species changed, whereas the other species remained constant. Firstly, keeping HQ concentration constant as 1×10^{-4} mol/L, DPVs of CC at different concentrations (Fig. 7A) were investigated. With increase of concentration, the oxidation peak of CC increased obviously. From the insert of Fig. 7A, it can be seen that the logarithm of the oxidation peak current of CC is linear with the logarithm of concentration in the range of 1×10^{-6} to 4×10^{-4} mol/L, and the regression equation is log I (μA) $=4.610+0.723$ log C (mol/L, $R=0.997$). The detection limit ($S/N=3$) was calculated as 2.0×10^{-7} mol/L for CC. Similarly, the DPVs of HQ with different concentrations in the presence of 1×10^{-4} mol/L CC (Fig. 7B) were also investigated and linear relationship was observed between the logarithm of the oxidation peak current and the logarithm of concentration in the range of 1×10^{-6} to 5×10^{-4} mol/L (Fig. 7B, inset). The regression equation was log I (μA)$=4.324+0.654$ log C (mol/L, $R=0.995$), and the detection limit ($S/N=3$) was 2.5×10^{-7} mol/L. The simultaneous determination of HQ and CC was demonstrated by changing their concentrations simultaneously. As shown in Fig. 7C, the current peak of HQ is separated from that of CC obviously, and the oxidation peaks were increase conformably. The logarithm of oxidation peak currents of HQ and CC increased linearly with the logarithm of concentration of their own in the range of 1.0×10^{-6} to 4.0×10^{-4} mol/L (Fig. 7C, inset). For CC (a), the regression equation is log I (μA)$=5.093+0.869$ log C (mol/L) and $R=0.992$, while for HQ (b), the regression equation is log I (μA)$=4.997+0.839$ log C (mol/L) and $R=0.991$. Compared with other electrochemical methods (Table 1), the proposed electrode shows rational linear range and acceptable detection of limit. From above studies, it is obvious that PDDA-G modified GCE is sensitive and efficient for the simultaneous detection of CC and HQ.

Table 2 Simultaneous determination results for CC and HQ in mixture water

Sample	Mixture water containing (1×10^{-5} mol/L)		Found (1×10^{-5} mol/L)		Recovery (%)	
	CC	HQ	CC	HQ	CC	HQ
1	5.00	5.00	4.95	4.90	98.9	98
2	7.00	7.00	6.86	7.17	97.9	102.4
3	10.00	10.00	10.31	9.82	103.1	98.2

Reproducibility of PDDA-G/GCE and interference studies

Eight modified electrodes were fabricated for the reproducibility studies. The mixture, containing 5×10^{-5} mol/L CC and 5×10^{-5} mol/L HQ, was determined under the optimized conditions by the eight modified electrodes. The relative standard deviation of the oxidation peak current was 5.4% for CC and 4.9% for HQ, respectively, indicating that the PDDA-G/GCE shows good reproducibility.

The influence of some possible interference in wastewater was investigated by analyzing a standard solution of 5.0×10^{-5} mol/L CC and HQ in pH 7.0 PBS. The 1,000-fold concentrations of K^+, Na^+, Cu^{2+}, Ca^{2+}, Mg^{2+}, Al^{3+}, NO_3^-, Cl^-, Ac^-, and SO_4^{2-} did not show interferences to the detection of CC and HQ. Moreover, 100-fold concentrations of resorcinol and 50-fold phenol did not show interference, too.

Sample analysis

Simultaneous determination of CC and HQ in Yellow River water, as a water sample after filtrating out sediment, was tested for the assessment of possible applications of the modified electrode. Since the amounts of HQ and CC were unknown in water samples, the spike and recovery experiments were performed by measuring the DPV responses to the samples in which the known concentrations of HQ and CC were added. The amounts of HQ and CC in the water sample were then determined by calibration method and the result was showed in Table 2. The recovery rate was in the range 97.9–103.1%. From there results, the electrode can be used for the detection of dihydroxybenzene isomers in real samples.

Conclusions

In this work, a modified GCE by PDDA-functionalized graphene nanosheets was fabricated and the electrochemical behaviors of CC and HQ on the modified electrode were investigated by using CV and DPV techniques. PDDA was employed to functionalize graphene nanosheets, and adsorbed onto the surface of graphene via the electrostatic interaction. After functionalization, the water solubility and the analyte adsorption of functionalized graphene were enhanced. The proposed method can completely separate the oxidation peaks of CC and HQ. Meanwhile, the proposed method exhibited many excellent performances, such as high sensitivity and selectivity, low detection limit, and wide linear range. Thus, it was very useful in the applications for quantitative determination of CC and HQ alone or mixed. In addition, satisfactory results were obtained when the proposed method was applied to determine CC and HQ in real water samples.

Acknowledgments The authors acknowledge the National Natural Science Foundation of China (20775030) for financial support of this work.

References

1. Xie T, Liu Q, Shi Y (2006) Simultaneous determination of positional isomers of benzenediols by capillary zone electrophoresis with square wave amperometric detection. J Chromatogr A 1109:317–321
2. Cui H, He CX, Zhao GW (1999) Determination of polyphenols by high-performance liquid chromatography with inhibited chemiluminescence detection. J Chromatogr A 855:171–179
3. Asan A, Isildak I (2003) Determination of major phenolic compounds in water by reversed-phase liquid chromatography after pre-column derivatization with benzoyl chloride. J Chromatogr A 988:145–149
4. Pistonesi MF, Nezio MSD, Centurión ME, Palomeque ME, Lista AG, Band BSF (2006) Determination of phenol, resorcinol and hydroquinone in air samples by synchronous fluorescence using partial least-squares (PLS). Talanta 69:1265–1268
5. Cui H, Zhang QL, Myint A, Ge XW, Liu LJ (2006) Chemiluminescence of cerium(IV)–rhodamine 6 G–phenolic compound system. J Photochem Photobiol A: Chem 181:238–245
6. Li SF, Li XZ, Xu J, Wei XW (2008) Flow-injection chemiluminescence determination of polyphenols using luminol–NaIO4–gold nanoparticles system. Talanta 75:32–37
7. Nagaraja P, Vasantha RA, Sunitha KR (2001) A sensitive and selective spectrophotometric estimation of catechol derivatives in pharmaceutical preparations. Talanta 55:1039–1046
8. Moldoveanu SC, Kiser M (2007) Gas chromatography/mass spectrometry versus liquid chromatography/fluorescence detection in the analysis of phenols in mainstream cigarette smoke. J Chromatogr A 1141:90–97
9. Garcia-Mesa JA, Mateos R (2007) Direct automatic determination of bitterness and total phenolic compounds in virgin olive oil using a ph-based flow-injection analysis system. J Agric Food Chem 55:3863–3868
10. Ding Y, Liu W, Wu Q, Wang X (2005) Direct simultaneous determination of dihydroxybenzene isomers at C-nanotube-modified electrodes by derivative voltammetry. J Electroanal Chem 575:275–280
11. Kong Y, Chen X, Wang W, Chen Zh (2011) A novel palygorskite-modified carbon paste amperometric sensor for catechol determination. Anal Chim Acta 688:203–207
12. Liu XY, Li YH, Liu XS, Zeng XD, Kong B, Luo SL, Wei WZ (2011) Simple sensor for simultaneous determination of dihydroxybenzene isomers. J Solid State Electrochem. doi:10.1007/s10008-011-1428-2
13. Peng J, Gao Z (2006) Influence of micelles on the electrochemical behaviors of catechol and hydroquinone and their simultaneous determination. Anal Bioanal Chem 384:1525–1532
14. Sun W, Jiang Q, Yang M, Jiao K (2008) Electrochemical behaviors of hydroquinone on a carbon paste electrode with ionic liquid as binder. Bull Kor Chem Soc 29:915–920
15. Zhang Y, Zheng JB (2007) Comparative investigation on electrochemical behavior of hydroquinone at carbon ionic liquid electrode, ionic liquid modified carbon paste electrode and carbon paste electrode. Electrochim Acta 52:7210–7216

16. Kheiri F, Sabzi R, Jannatdoust E, Sedghi H (2010) Acetone extracted propolis as a novel membrane and its application in phenol biosensors: the case of catechol. J Solid State Electrochem. doi:10.1007/s10008-010-1250-2
17. Zhao D, Zhang X, Feng L, Jia L, Wang S (2009) Simultaneous determination of hydroquinone and catechol at PASA/MWNTs composite film modified glassy carbon electrode. Colloid Surf B 74:317–321
18. Wang L, Huang P, Bai J, Wang H, Zhang L, Zhao Y (2007) Covalent modification of a glassy carbon electrode with penicillamine for simultaneous determination of hydroquinone and catechol. Microchim Acta 158:151–157
19. Qi H, Zhang C (2005) Simultaneous determination of hydroquinone and catechol at a glassy carbon electrode modified with multiwall carbon nanotubes. Electroanalysis 17:832–838
20. Yu J, Du W, Zhao F, Zeng B (2009) High sensitive simultaneous determination of catechol and hydroquinone at mesoporous carbon CMK-3 electrode in comparison with multi-walled carbon nanotubes and Vulcan XC-72 carbon electrodes. Electrochim Acta 54:984–988
21. Yang P, Zhu Q, Chen Y, Wang F (2009) Simultaneous determination of hydroquinone and catechol using poly(*p*-aminobenzoic acid) modified glassy carbon electrode. J Appl Polymer Sci 113:2881–2886
22. Ahammad A, Sarker S, Rahman M, Lee J (2010) Simultaneous determination of hydroquinone and catechol at an activated glassy carbon electrode. Electroanalysis 22:694–700
23. Ghanem MA (2007) Electrocatalytic activity and simultaneous determination of catechol and hydroquinone at mesoporous platinum electrode. Electrochem Commun 9:2501–2506
24. Wang Z, Li S, Lv Q (2007) Simultaneous determination of dihydroxybenzene isomers at single-wall carbon nanotube electrode. Sens Actuators B 127:420–425
25. Zhang D, Peng Y, Qi H, Gao Q, Zhang C (2009) Application of multielectrode array modified with carbon nanotubes to simultaneous amperometric determination of dihydroxybenzene isomers. Sens Actuators B 136:113–121
26. Du HJ, Ye JS, Zhang JQ, Huang XD, Yu CZ (2011) A voltammetric sensor based on graphene-modified electrode for simultaneous determination of catechol and hydroquinone. J Electroanal Chem 650:209–213
27. Singh R (2010) Thin films of Pd and Pd–1% MWCNT as new electrocatalysts for oxidation of phenol in acid medium. J Solid State Electrochem 14:2113–2120
28. Yin HS, Zhang QM, Zhou YL, Ma Q, Liu T, Zhu LS, Ai SY (2011) Electrochemical behavior of catechol, resorcinol and hydroquinone at graphene–chitosan composite film modified glassy carbon electrode and their simultaneous determination in water samples. Electrochim Acta 56:2748–2753
29. Schedin F, Geim AK, Morozov SV, Hill EW, Blake P, Katsnelson MI, Novoselov KS (2007) Detection of individual gas molecules adsorbed on graphene. Nat Mater 6:652–655
30. Tang LH, Wang Y, Li YM, Feng HB, Lu J, Li JH (2009) Preparation, structure, and electrochemical properties of reduced graphene sheet films. Adv Funct Mater 19:2782–2789
31. Yin HS, Zhou YL, Cui L, Liu T, Ju P, Zhu LS, Ai SY (2011) Sensitive voltammetric determination of rutin in pharmaceuticals, human serum, and traditional Chinese medicines using a glassy carbon electrode coated with graphene nanosheets, chitosan, and a poly(amido amine) dendrimer. Microchim Acta 173:337–345
32. Zhang FY, Li YJ, Gu YE, Wang ZH, Wang CM (2011) One-pot solvothermal synthesis of a Cu2O/Graphene nanocomposite and its application in an electrochemical sensor for dopamine. Microchim Acta 173:103–109
33. Niyogi S, Bekyarova E, Itkis ME, McWilliams JL, Hamon MA, Haddon RC (2006) Soluation properties of graphite and graphene. J Am Chem Soc 24:7720–7721
34. Liu KP, Zhang JJ, Yang GH, Wang CM, Zhu JJ (2010) Direct electrochemistry and electrocatalysis of hemoglobin based on poly (diallyldimethylammonium chloride) functionalized graphene sheets/room temperature ionic liquid composite film. Electrochem Commun 12:402–405
35. Xu ZA, Gao N, Dong SJ (2006) Preparation and layer-by-layer self-assembly of positively charged multiwall carbon nanotubes. Talanta 68:753–758
36. Hummers WS, Offeman RE (1958) Preparation of graphitic oxide. J Am Chem Soc 6:1339
37. Niu JJ, Wang JN (2008) Activated carbon nanotubes-supported catalyst in fuel cells. Electrochim Acta 53:8058–8063
38. Laviron E (1979) General expression of the linear potential sweep voltammogram in the case of diffusionless electrochemical systems. J Electroanal Chem 101:19–28
39. Gulaboski R, Lovric M, Mirceski V, Bogeski I, Hoth M (2008) A new rapid and simple method to determine the kinetics of electrode reactions of biologically relevant compounds from the half-peak width of the square-wave voltammograms. Biophys Chem 138:130–137
40. Zhang Y, Zeng GM, Tang L, Huang DL, Jiang XY, Chen YN (2007) A hydroquinone biosensor using modified core–shell magnetic nanoparticles supported on carbon paste electrode. Biosens Bioelectron 22:2121–2126